

Electronic interferometer capacitively coupled to a quantum dot

Seok-Chan Youn,¹ Hyun-Woo Lee,² and H.-S. Sim¹

¹*Department of Physics, Korea Advanced Institute of Science and Technology, Daejeon 305-701, Korea*

²*PCTP and Department of Physics, Pohang University of Science and Technology, Pohang 790-784, Korea*

(Received 1 December 2008; revised manuscript received 4 July 2009; published 24 September 2009)

We theoretically study electron interference in a ballistic electronic interferometer capacitively coupled to a quantum dot. The visibility of the interference is reduced when the dot has degenerate ground states with different excess charges. The degree of the reduction depends on system parameters such as the strength of the capacitive coupling, and the dependence is analyzed in the regime where the dwell time of electrons in the dot is much longer than the electron flight time through the interferometry region coupled to the dot. The result is consistent with recent experimental data.

DOI: 10.1103/PhysRevB.80.113307

PACS number(s): 73.23.-b, 03.65.Yz, 85.35.Ds

I. INTRODUCTION

Electronic interference is one of the main issues in mesoscopic physics. It has been experimentally studied in various systems such as a quantum ring^{1,2} and an electronic Mach-Zehnder interferometer (EMZI).³⁻⁵

The interference is reduced by the dephasing and by the phase averaging. In the dephasing, an electron loses its phase due to the interactions with other particles during its propagation along interference paths. Electron-electron interaction is known to be the main source of the dephasing at low temperature. The properties of the interaction-induced dephasing vary from systems to systems.⁶⁻¹² On the other hand, in the phase averaging, each electron does not lose its phase but experiences a different phase shift. Then, the measured interference signal, which is the average over electrons, can be suppressed. The phase averaging appears even in noninteracting systems under a finite bias voltage or at finite temperature, as electrons in the finite energy window have different momentum and thus different phase shifts.

Recently, Meier and the co-workers experimentally investigated a quantum ring capacitively coupled to a quantum dot in the Coulomb blockade regime.² They measured the amplitude of the Aharonov-Bohm interference of the ring, and simultaneously detected electron current along a separate circuit containing the dot. The amplitude shows a dip, when the dot has degenerate states with different excess charges and thus shows a Coulomb blockade peak of electron conductance. The dip was qualitatively explained² as the phase averaging, in which the phase accumulation of an electron along the ring depends on the occupation of the dot. A quantitative analysis of the interference reduction, which has not been reported yet and is the aim of the present work, will be interesting and useful, as it comes from charge fluctuations in a *single* resonance level, rather than those in macroscopic systems, thus contains the information of the resonance. Note that there have been a theoretical study⁶ on the dephasing due to a macroscopic gate nearby the interferometer, and lots of studies¹³ on the properties (such as decoherence) of the dot affected by its capacitive coupling to a conducting wire.

In this Brief Report, we consider an electronic interferometer (Fig. 1) capacitively coupled to a quantum dot in the

Coulomb blockade regime, and study the reduction of the interference visibility \mathcal{V} due to the charge fluctuation of the dot; other sources⁶ of the reduction are omitted here. We focus on the regime of $t_{fl} \ll \tau_{dwell}$, where the reduction results from the phase averaging rather than the dephasing. Here, τ_{dwell} and t_{fl} are electron dwell time of the dot and electron flight time t_{fl} through the interferometer region coupled to the dot, respectively.

We derive the visibility \mathcal{V} in the linear response regime, based on a self-consistent treatment of the interaction, and obtain the dependence of \mathcal{V} on temperature $k_B T$, gate voltage V_G applied to the dot, and interaction strength parameter g [defined below Eq. (3)]. The visibility shows a dip when the dot shows a Coulomb blockade resonance. The depth of the dip is governed by g while the width is determined mainly by $k_B T$. The width is comparable with that of the Coulomb

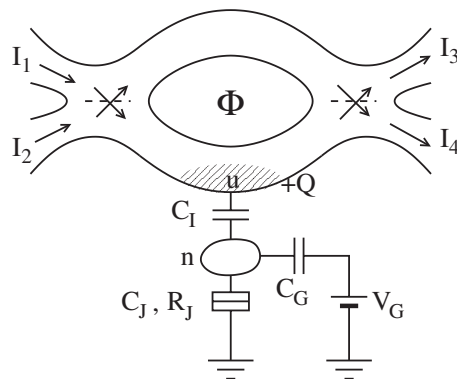


FIG. 1. Schematic diagram of an electronic interferometer capacitively coupled to a quantum dot. It couples to four reservoirs via two beam splitters (dashed lines) and has two arms enclosing magnetic flux Φ . Here, multiple circulation paths along the interference loop are ignored; thus the setup can be regarded as a Mach-Zehnder type. The dot is in the Coulomb blockade regime and capacitively couples to a (shady) region of the lower arm (with capacitance C_1) and to a macroscopic gate (with C_G). Voltage V_G is applied to the gate. The dot also connects to an electron reservoir via tunneling junction with junction resistance R_J and capacitance C_J . The fluctuation of charge ne in the dot causes that of induced charge Q and potential u in the coupling region of the lower arm, resulting in the reduction of the interference visibility.

blockade conductance peak of the dot. These results are in good agreement with the experimental data.²

Our setup is shown in Fig. 1. Source-drain bias voltage V_{sd} is applied to reservoir 1. Each arm of the interferometer is modeled by a disorder-free single-channel quantum wire with length L and the Fermi velocity v_F . The length of the interferometer region coupled to the dot is denoted as l . The dot is considered to be in the metallic Coulomb blockade regime where its single-particle level spacing is much smaller than $k_B T$. In this regime, $E_C \gg k_B T$, \hbar/τ_{dwell} and $R_J \gg R_0$, where $R_0 \equiv h/e^2$ and $E_C = e^2/C_{tot}$ is the charging energy of the dot [see Eq. (5)]. We make the following simplifications. We ignore multiple circulation paths around the interference loop, thus our model can describe an EMZI. In the regime of $\tau_{dwell} \gg t_{fl}(=l/v_F)$, the potential u of the coupling region can be approximated⁶ to be position independent over the length l . We ignore the effect of C_J , since it is rather trivial, and will briefly discuss it later.

We remark that under the above simplifications, the RC time τ_{RC} in the coupling region is much shorter than τ_{dwell} , since $\tau_{RC} = R_0 C_{eff} < R_0 C_{tot} = h/E_C$ and $E_C \gg \hbar/\tau_{dwell}$, where $C_{eff} \equiv C_G C_1 / (C_G + C_1)$ is the effective capacitance between the coupling region and the gate.

II. POTENTIAL FLUCTUATION

The fluctuation of the potential u at the coupling region affects the interference visibility. Below, we obtain u , by solving self-consistent equations relating u , the induced charge Q in the coupling region, and the excess charge $-ne$ of the dot. We note that Q is well defined in our regime of $\tau_{RC} \ll \tau_{dwell}$ and that the same approach was used in Ref. 6 where an interferometer capacitively coupled to a macroscopic gate is considered.

In the frequency domain, Q is related to the dot charge $-ne$ and also to the bias voltage V_{sd} , V_G ,

$$Q(\omega) = C_{eff} \left[u(\omega) - V_G(\omega) + \frac{en(\omega)}{C_G} \right], \quad (1)$$

$$Q(\omega) = e^2 \nu(\omega) [V_{sd}(\omega) - N_{res} u(\omega)]. \quad (2)$$

Here, N_{res} is the number of the reservoirs from which an electron can move into the coupling region. It depends on the interferometer setup; in the EMZI,³ the channels in the coupling region are chiral, thus, $N_{res} = 2$, while in a ring coupled to four reservoirs, the channels are not chiral and $N_{res} = 4$. The injectivity $\nu(\omega)$ is the density of states of the electron entering from a reservoir to the coupling region via the beam splitter in between.¹⁴ For simplicity, we have fixed the transmission probabilities of the beam splitters to be 0.5 so that the N_{res} reservoirs have the same injectivity, $\nu(\omega) = i(1 - e^{i\omega t_{fl}})/(2\hbar\omega)$. The origin of Eq. (2) is the fact that electron flow occurs between the reservoirs and the coupling region, to screen excess charges; the second term of Eq. (2) describes the screening. From Eqs. (1) and (2), one finds

$$u(\omega) = \frac{(1 - g^2)\nu(\omega) \frac{V_{sd}(\omega)}{N_{res}} + g^2\nu(0) \left[V_G(\omega) - \frac{en(\omega)}{C_G} \right]}{(1 - g^2)\nu(\omega) + g^2\nu(0)}. \quad (3)$$

Here, $g^2 \equiv C_{eff}/(C_{eff} + e^2 D)$ is the dimensionless (Luttinger) parameter¹⁵ representing interaction strength at the coupling region, and $D = N_{res}\nu(0) = N_{res}t_{fl}/2\hbar$ is the density of states of the coupling region.

For $\tau_{RC}, t_{fl} \ll \tau_{dwell}$, Eq. (3) predicts the following behavior of the time dependence $u(t)$. When an electron tunnels into the dot so that n changes from one integer n_0 to $n_0 + 1$, $u(t)$ jumps from u_{n_0} (value before the tunneling), oscillates around $u_{n_0 + 1}$, and finally stabilizes to $u_{n_0 + 1}$. The oscillation decays roughly¹⁶ within the time scale of τ_{RC} . The stabilization value $u_n = u(\omega = 0)$ is

$$u_n = (1 - g^2)(V_{sd}/N_{res}) + g^2[V_G - en/C_G]. \quad (4)$$

Here, we ignore the fluctuation of the applied voltages V_{sd} and V_G , which is valid⁶ in the case that the external circuit connected to the interferometer has no impedance. In the regime of $t_{fl} \ll \tau_{dwell}$, an interfering electron in the setup feels the stabilization value u_n of the potential most of time so that the interference visibility is determined by the discrete values u_{n_0} and $u_{n_0 + 1}$ (see the next section). In contrast, as the system goes beyond the regime $t_{fl} \ll \tau_{dwell}$, the visibility becomes affected by the variation of $u(t)$ between the stabilization values.

Using $Q(\omega) = C_1[u(\omega) - V_{dot}(\omega)]$, one also finds the electrostatic potential V_{dot} of the dot as $V_{dot}(\omega = 0) = [(C_G + g^2 C_1)(V_G - en/C_G) + C_1(1 - g^2)V_{sd}/N_{res}]/(C_G + C_1)$, when the dot has n excess electrons. Then, the energy $E_D = \int_0^n dn' (-e)V_{dot}(n')$ of the dot is obtained as

$$E_D = \frac{(ne - Q_0)^2}{2C_{tot}} + (\text{terms independent of } ne), \quad (5)$$

the total capacitance of the dot is found to be $C_{tot} = C_G(C_G + C_1)/(C_G + g^2 C_1)$, and the effective gate charge is $Q_0 = C_G V_G + (1 - g^2)C_1 C_G V_{sd}/[N_{res}(C_G + g^2 C_1)]$. This result is understood from the fact that u is affected not only by the external voltages but also by screening.

It is worthwhile to discuss two limiting cases of $g \rightarrow 1$ and $g \rightarrow 0$. The weak coupling limit of $g \rightarrow 1$ occurs when $C_{eff} \gg e^2 D$ (i.e., $\tau_{RC} \gg t_{fl}$). In this limit, the charge fluctuation in the coupling region does not affect u , thus $u \rightarrow V_G - en/C_G$ (independent of V_{sd}), $V_{dot} \rightarrow u$ (no charge accumulation in C_1), and $C_{tot} (= e^2/E_C) \rightarrow C_G$. On the other hand, in the strong coupling limit of $g \rightarrow 0$, u is governed by n and V_{sd} , and $C_{tot} \rightarrow C_G + C_1$.

For later use, we discuss the probability P_n that the dot has n electrons. In the Coulomb blockade regime, the dot states can be described by only two occupation numbers, saying $n \in \{n_0, n_0 + 1\}$, and have the energy $E_D(n)$. The probability P_n is obtained^{17,18} from the stationary conditions, $P_{n_0} \Gamma^+ = P_{n_0 + 1} \Gamma^-$ and $P_{n_0} + P_{n_0 + 1} = 1$, as

$$P_{n_0} = \frac{1}{1 + e^{\Delta_E/k_B T}}, \quad P_{n_0+1} = \frac{1}{1 + e^{-\Delta_E/k_B T}}. \quad (6)$$

Here, Γ^+ (Γ^-) is the rate of the transition $n_0 \rightarrow n_0+1$ ($n_0+1 \rightarrow n_0$), $\Gamma^\pm = \pm \Delta_E/[e^2 R_J(1 - e^{\mp \Delta_E/k_B T})]$, and $\Delta_E = E_D(n_0) - E_D(n_0+1) = e^2(Q_0/e - n_0 - 1/2)/C_{\text{tot}}$ is the energy difference between the two states of n_0 and n_0+1 . The dwell time τ_{dwell} of the dot can be estimated by \hbar/Γ^+ for the state with n_0 (\hbar/Γ^- for n_0+1).

III. SLOW FLUCTUATION REGIME

In this section, the visibility of the interference in the current through the interferometer is derived and analyzed in the regime of $t_{\text{fl}} \ll \tau_{\text{dwell}}$.

In the linear response regime, electron current from the source reservoir 1 to 3 (one of the drains) can be described by the Landauer-Büttiker formula. The differential conductance is given by $G_{13} = (e^2/h) \int dE (-\partial f/\partial E) \langle T_{13}(E) \rangle$. Here, $T_{13}(E)$ is the transmission probability of an electron with energy E from the reservoir 1 to 3, and $\langle \dots \rangle$ denotes the statistical average over the fluctuation of u .

In the regime of $t_{\text{fl}} \ll \tau_{\text{dwell}}$, the occupation number of the dot does not fluctuate most of time while an interfering electron passes through the coupling region. In this case, and when the dot has n excess electrons, u has the stabilization value u_n in Eq. (4), and the resulting transmission probability $T_{13;n}$ has the form of

$$T_{13;n}(E) = \frac{1}{2} \{1 + \cos[-2\pi\Phi/\Phi_0 + \Theta_n]\}, \quad (7)$$

where $2\pi\Phi/\Phi_0$ is the Aharonov-Bohm phase, $\Phi_0 = h/e$, and $\Theta_n = -eu_n t_{\text{fl}}/\hbar$ is the phase shift induced by the potential u_n ; here, the lengths of the two arms of the setup are assumed to be identical so that the dynamical phase is absent in $T_{13;n}$. At the gate voltage where the probability P_n is not negligible only for $n \in \{n_0, n_0+1\}$ [see Eq. (6)], one obtains the ensemble average of $T_{13;n}$ over the possible values of n , $\langle T_{13}(E) \rangle = \sum_{n=n_0, n_0+1} P_n T_{13;n}(E)$, and the visibility $\mathcal{V} \equiv [\max(G_{13}) - \min(G_{13})]/[\max(G_{13}) + \min(G_{13})]$ of the interference in G_{13} ,

$$\mathcal{V} = \left| \sum_n P_n e^{-i\Theta_n} \right| = \sqrt{1 - \frac{2\Gamma^+\Gamma^-(1 - \cos \Delta\phi)}{(\Gamma^+ + \Gamma^-)^2}}, \quad (8)$$

$$\Delta\phi \equiv \Theta_{n_0+1} - \Theta_{n_0} = \frac{4\pi(1-g^2)}{N_{\text{res}}} \frac{C_1}{C_G + C_1}, \quad (9)$$

where $\max(G_{13})$ ($\min(G_{13})$) is the maximum (minimum) value of G_{13} in one Aharonov-Bohm period and $\Delta\phi$ is the phase difference between the two cases of n_0 and n_0+1 . Hereafter, we put $N_{\text{res}}=2$, by considering an EMZI.³

In Fig. 2(a), we plot the visibility \mathcal{V} as a function of V_G . Around the Coulomb blockade resonance of $\Delta_E=0$, where the occupation number of the dot maximally fluctuates ($P_{n_0} = P_{n_0+1}=0.5$), $\mathcal{V}(V_G)$ shows a dip. The dip center occurs at the gate voltage of $Q_0 = e(n_0+1/2)$. The depth d and the width V_{width} of the dip are

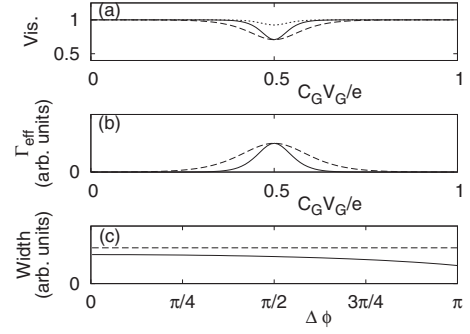


FIG. 2. (a) Visibility \mathcal{V} and (b) effective transition rate Γ of the dot, as a function of V_G , in the regime of $t_{\text{fl}} \ll \tau_{\text{dwell}}$. V_G varies around the Coulomb blockade resonance where the dot has $n_0=0$ or $(n_0+1)=1$ electrons. Different values of temperature $t=k_B T/E_c$ and phase difference $\Delta\phi$ are considered: $(t, \Delta\phi) = (0.05, \pi/2)$ [see full line], $(0.1, \pi/2)$ [dashed], and $(0.05, \pi/4)$ [dotted]. We put $N_{\text{res}}=2$. (c) The width of the dip of \mathcal{V} in (a) as a function of $\Delta\phi$ [see full line]. It is found to weakly depend on $\Delta\phi$. For comparison, we also draw the width of the peak of Γ_{eff} in (b) [dashed]; it is independent of $\Delta\phi$. The sizes of the two widths are comparable.

$$d = 1 - \left| \cos \frac{\Delta\phi}{2} \right|, \quad eV_{\text{width}} = 2\xi k_B T, \quad (10)$$

where $\xi = \log(1+\eta)/(1-\eta)$,

$$\eta = \sqrt{3/4 - (1 - \cos(\Delta\phi/2))/(1 - \cos \Delta\phi)};$$

note that $\mathcal{V} = |\cos(\Delta\phi/2)|$ at the dip center. The depth is independent of $k_B T$, and becomes larger for stronger interaction. The dip (i.e., the reduction in the visibility) disappears in the weak coupling limit of $g \rightarrow 1$, while $d \rightarrow 1 - \cos[(2\pi/N_{\text{res}})C_1/(C_G + C_1)]$ in the strong coupling limit of $g \rightarrow 0$. The width V_{width} linearly increases with the increase in the temperature, and depends weakly on g ; as $\Delta\phi$ changes from 0 to π , ξ varies from 1.76 to 1.10.

On the other hand, the linear response conductance of a circuit including the dot is known^{17,18} to be proportional to the effective transition rate $\Gamma_{\text{eff}} \equiv \Gamma^+\Gamma^-/(\Gamma^+ + \Gamma^-)$. As a function of the gate voltage, it shows a peak at the Coulomb blockade resonance. The width of the peak is proportional to the temperature; the full width at half maximum is given by $4.35k_B T/e$. Interestingly, the width of the conductance peak is comparable to that of the visibility dip [Fig. 2(c)]. This finding is in good agreement with the experimental result² of the visibility dips and the conductance peaks.

The mechanism of the above visibility reduction is the phase averaging. In the regime of $t_{\text{fl}} \ll \tau_{\text{dwell}}$, each interfering electron does not lose its phase while it passes along the coupling region, but its phase is either Θ_{n_0} or Θ_{n_0+1} , depending on the occupation of the dot. The average over the different phases cause the reduction in the interference signal. This behavior is in contrast to the similar case⁶ of an interferometer coupled a macroscopic gate. In this case, the reduction mechanism is the dephasing due to thermal charge fluctuations, and the details such as the temperature dependence of the reduction are different from our result.

We note that the qualitatively same result is obtained for a semiconductor dot where only one single-particle level is relevant. And, multiple circulation paths along the interference loop, ignored in our work, will not modify the above result qualitatively, as far as the time scales of the multiple circulations of an electron along the loop are not much longer than τ_{dwell} . This guarantees the agreement between our result for the EMZI and the experimental data² for a ring.

In addition, our result is only qualitatively modified in a more realistic case with finite C_J and a direct capacitance C_D between the coupling region and the gate. In the presence of C_J and C_D , Eq. (9) is modified by the replacements, $g^2 \equiv C_{\text{eff}}/(C_{\text{eff}}+e^2D) \rightarrow C'_{\text{eff}}/(C'_{\text{eff}}+e^2D)$, $C_{\text{eff}} \equiv C_G C_I/(C_G+C_I) \rightarrow C'_{\text{eff}} \equiv C_D+C_G(C_I+C_J)/(C_G+C_I+C_J)$, and $C_G+C_I \rightarrow C_G+C_I+C_J$ in the denominator. The modifications in other capacitance-dependent quantities of Q_0 and C_{tot} (not shown here) does not affect our main results in Eqs. (9) and (10) and in Fig. 2.

Finally, we briefly discuss the case that the system deviates from the regime of $t_{\text{fl}} \ll \tau_{\text{dwell}}$; this case is the strong coupling regime of $g \ll 1$ (i.e., $t_{\text{fl}} \gg \tau_{\text{RC}}$) under the Coulomb blockade condition of $\tau_{\text{dwell}} \gg \tau_{\text{RC}}$. In this case, one has to take into account of the fluctuation of $u(t)$ over the flight time t_{fl} , thus our approach should be modified. For example, for $\tau_{\text{dwell}} \gg t_{\text{fl}}$, the visibility and the dephasing rate may be approximately obtained, as in Ref. 6, by studying the fluctuation spectra of u and n , and they will deviate from Eqs. (8)–(10) due to the additional dephasing induced by the de-

pendence of u on time. Note that the fluctuation spectra will be affected by the backaction from $u(t)$ to $n(t)$ except for $C_I \ll C_G$. On the other hand, the limiting case of $t_{\text{fl}} \gg \tau_{\text{dwell}}$ is likely to be hardly found in a realistic situation such as in Ref. 2. For this case, our assumption that u has no spatial dependence over the coupling region is not valid, and other approaches¹⁵ may be helpful.

IV. CONCLUSIONS

We have investigated the reduction in the interference visibility in an electronic interferometer capacitively coupled to a quantum dot. The reduction appears when the dot shows Coulomb blockade resonances. The features of the resonant reduction in the visibility are different from the dephasing effect in an interferometer coupled to a macroscopic gate. Our result of the visibility reduction can be used for the detection of single charges, and provide a model for a local charge trap^{4,19} (unintentionally) formed nearby an electronic interferometer.

ACKNOWLEDGMENTS

We thank M. Büttiker for useful discussion, and KRF (Grant No. 2006-331-C00118), NRF (Grant No. 2009-0078437), and MOST (the leading basic S & T research projects) for support.

-
- ¹A. E. Hansen, A. Kristensen, S. Pedersen, C. B. Sorensen, and P. E. Lindelof, Phys. Rev. B **64**, 045327 (2001).
²L. Meier, A. Fuhrer, T. Ihn, K. Ensslin, W. Wegscheider, and M. Bichler, Phys. Rev. B **69**, 241302(R) (2004).
³Y. Ji *et al.*, Nature (London) **422**, 415 (2003); I. Neder, M. Heiblum, Y. Levinson, D. Mahalu, and V. Umansky, Phys. Rev. Lett. **96**, 016804 (2006); I. Neder *et al.*, Nat. Phys. **3**, 534 (2007).
⁴L. V. Litvin, H.-P. Tranitz, W. Wegscheider, and C. Strunk, Phys. Rev. B **75**, 033315 (2007); L. V. Litvin, A. Helzel, H. P. Tranitz, W. Wegscheider, and C. Strunk, *ibid.* **78**, 075303 (2008).
⁵P. Roulleau, F. Portier, D. C. Glatli, P. Roche, A. Cavanna, G. Faini, U. Gennser, and D. Mailly, Phys. Rev. B **76**, 161309(R) (2007); P. Roulleau, F. Portier, P. Roche, A. Cavanna, G. Faini, U. Gennser, and D. Mailly, Phys. Rev. Lett. **100**, 126802 (2008); **101**, 186803 (2008).
⁶G. Seelig and M. Büttiker, Phys. Rev. B **64**, 245313 (2001); M. Büttiker and A. M. Martin, *ibid.* **61**, 2737 (2000).
⁷K. Le Hur, Phys. Rev. Lett. **95**, 076801 (2005).
⁸Jaek U. Kim, W.-R. Lee, Hyun-Woo Lee, and H.-S. Sim, Phys. Rev. Lett. **102**, 076401 (2009).
⁹S.-C. Youn, H.-W. Lee, and H.-S. Sim, Phys. Rev. Lett. **100**, 196807 (2008).
¹⁰I. Neder and E. Ginossar, Phys. Rev. Lett. **100**, 196806 (2008).
¹¹I. Neder and F. Marquardt, N. J. Phys. **9**, 112 (2007).

- ¹²E. V. Sukhorukov and V. V. Cheianov, Phys. Rev. Lett. **99**, 156801 (2007); I. P. Levkivskyi and E. V. Sukhorukov, Phys. Rev. B **78**, 045322 (2008).
¹³M. Field, C. G. Smith, M. Pepper, D. A. Ritchie, J. E. F. Frost, G. A. C. Jones, and D. G. Hasko, Phys. Rev. Lett. **70**, 1311 (1993); A. Yacoby, M. Heiblum, D. Mahalu, and H. Shtrikman, *ibid.* **74**, 4047 (1995); H. Aikawa, K. Kobayashi, A. Sano, S. Katsumoto, and Y. Iye, *ibid.* **92**, 176802 (2004).
¹⁴M. Büttiker, J. Phys.: Condens. Matter **5**, 9361 (1993).
¹⁵Y. M. Blanter, F. W. J. Hekking, and M. Büttiker, Phys. Rev. Lett. **81**, 1925 (1998).
¹⁶In the strong coupling regime ($g \ll 1$), the decay takes longer time than τ_{RC} in our model. It may be the artifact of the simplification that the spatial dependence of u is ignored. Even in this case, the phase shift $\int^n dt' u(t')$ stabilizes within τ_{RC} , and thus the effect of the longer decay on the visibility is negligible in the case of $t_{\text{fl}} \ll \tau_{\text{dwell}}$.
¹⁷A. N. Korotkov, Phys. Rev. B **49**, 10381 (1994).
¹⁸Y. Utsumi, Phys. Rev. B **75**, 035333 (2007).
¹⁹L. V. Litvin *et al.*, Physica E **40**, 1706 (2008); A. Pioda, S. Kicin, D. Brunner, T. Ihn, M. Sigrist, K. Ensslin, M. Reinwald, and W. Wegscheider, Phys. Rev. B **75**, 045433 (2007); S. Kafanov, H. Brenning, T. Duty, and P. Delsing, Phys. Rev. B **78**, 125411 (2008).